Chapter 3. Fabrication and characterization of (1-x)$SrBi_2Ta_2O_9$-xBi_3TaTiO_9 layered structure solid solution thin films for FRAM applications

In this chapter, the optimization process of (1-x)$SrBi_2Ta_2O_9$-xBi_3TaTiO_9 layered structure solid solution thin films is discussed. The electrical and ferroelectric properties of the solid solution thin films with x=0.1-0.5 were obtained and compared to find the best compositional solid solution thin films for the ferroelectric nonvolatile memory applications. Also, some of the representative properties of a optimized compositional solid solution thin films are exhibited.

3.1 ABSTRACT

We report on the properties of (1-x)$SrBi_2Ta_2O_9$-xBi_3TaTiO_9 solid solution thin films for ferroelectric non-volatile memory applications. The solid solution thin films fabricated by modified metalorganic solution deposition technique showed much improved properties compared to $SrBi_2Ta_2O_9$. A pyrochlore free crystalline phase was obtained at a low annealing temperature of 600 ^{o}C and grain size was found to be considerably increased for the solid solution compositions. The film properties were found to be strongly dependent on the composition and annealing temperatures. The measured dielectric constant of the solid solution thin films was in the range 180-225 for films with 10-50 % of Bi_3TaTiO_9 content in the solid solution. Ferroelectric properties of (1-x)$SrBi_2Ta_2O_9$-xBi_3TaTiO_9 thin films were significantly improved compared to $SrBi_2Ta_2O_9$. For example, the observed $2P_r$ and E_c values for films with 0.7$SrBi_2Ta_2O_9$-0.3Bi_3TaTiO_9 composition, annealed at 650 ^{o}C, were 12.4 μC/cm^2 and 80 kV/cm, respectively. The solid solution thin films showed less than 5 % decay of the polarization charge after 10^{10} switching cycles and good memory retention characteristics after about 10^6 s of memory retention. The improved microstructural and ferroelectric properties of (1-x)$SrBi_2Ta_2O_9$-xBi_3TaTiO_9 thin films compared to $SrBi_2Ta_2O_9$, especially at lower annealing temperatures, suggest their suitability for high density FRAM applications.

3.2. INTRODUCTION

Integration of ferroelectric thin films into nonvolatile memory has drawn great attention to computer industry [1-3]. Their superior performance in writing speed and radiation hardness over other storage devices such as magnetic core and magnetoinductive plated wire memories, floating and flash erasable programmable read only memories (EEPROMs) has already been demonstrated [4,5]. Among the ferroelectric materials, $Pb(Zr_xTi_{1-x})O_3$ and $SrBi_2Ta_2O_9$ thin films have been extensively studied because of their good ferroelectric properties. Despite good ferroelectric switching properties, the degradation of the polarization state of the $Pb(Zr_xTi_{1-x})O_3$ capacitors with platinum electrodes has been a major obstacle in realizing a practical memory device [6-8]. This problem has been overcome by using complex metal-oxide electrodes [9,10], however, the $Pb(Zr_xTi_{1-x})O_3$ capacitors fabricated on these electrodes have shown higher leakage current and the film/electrode interface is usually non-ohmic. Recently, $SrBi_2Ta_2O_9$ thin films have attracted a lot of attention because of fatigue free polarization switching characteristics on simple metal electrodes [11-13]. In addition, $SrBi_2Ta_2O_9$ thin films show good ferroelectric properties and low leakage current even for very small thicknesses. However, the integration of $SrBi_2Ta_2O_9$ thin films as a device component has been delayed due to problems of high processing temperature (> 700 ^oC), relatively low P_r for high density applications, and low Curie temperature (T_c) for high temperature applications. High remanent polarization may not be critical provided that the ferroelectric properties are well defined. But, high temperature processing of oxide thin film causes serious deterioration of the ferroelectric film/electrode interface characteristics [14]. For high density application, the ferroelectric films are required to be deposited directly on poly-silicon [15], for which a low temperature processing is required to maintain good interfacial properties.

It has not been possible to obtain good ferroelectric properties on $SrBi_2Ta_2O_9$ thin films at temperatures lower than 700 ^oC because of small grain sizes. It has been established that a critical grain size is required to get good ferroelectric properties on $SrBi_2Ta_2O_9$ thin films [16-17] and annealing at temperatures higher than 650 ^oC is necessary, under normal pressure conditions, to obtain the critical grain size. Several attempts have been made to improve the microstructure and, hence, the ferroelectric properties of $SrBi_2Ta_2O_9$ thin films at lower annealing temperatures either by making the Sr/Bi/Ta atomic ratio slightly off-stoichiometric [18] or by annealing the

films under low oxygen pressure environment [19]. However, it has not been possible to obtain good electrical properties at lower annealing temperatures. In the present work, we have made an attempt to enhance the grain growth at lower annealing temperature and, hence, improve the ferroelectric properties by using a solid solution of layered perovskite materials. The solid solution of different materials has been a common approach for bulk materials to modify phases and properties of the system. In the present study Bi_3TaTiO_9, which belongs to layered perovskite family, was chosen for the solid solution based on the following considerations: (1) The solid solution of $SrBi_2Ta_2O_9$-Bi_3TaTiO_9 system was first established by Subbarao [20] based on the x-ray powder diffraction studies and Zhang *et al.* analyzed the solubility of Bi_3TiNbO_9 into $SrBi_2Ta_2O_9$ system and concluded that for Bi_3TiNbO_9 content up to 60%, $SrBi_2Ta_2O_9$ acts as host material [21], (2) T_c in the range 870-920 ^oC has been reported for bulk Bi_3TaTiO_9 material [20]. So the solid solution of $SrBi_2Ta_2O_9$ and Bi_3TaTiO_9 is expected to show higher Curie temperature, (3) A linear T_c-P_s dependence has been reported for materials belonging to layered perovskite family [22]. Therefore an improvement in the ferroelectric properties is expected for the solid solution compositions with higher Curie temperature than $SrBi_2Ta_2O_9$. In the present paper, we report on the microstructural and electrical properties of (1-x)$SrBi_2Ta_2O_9$-xBi_3TiTaO_9 solid solution thin films. The electrical properties reported include dielectric, ferroelectric, and leakage current characteristics. The effects of annealing temperature on the phase development and electrical properties have also been analyzed.

3.3. EXPERIMENTAL PROCEDURE

Thin films of (1-x)$SrBi_2Ta_2O_9$-xBi_3TiTaO_9 solid solution were prepared by the modified metalorganic solution deposition technique using a room temperature processed alkoxide-carboxylate precursor solution [23]. For the preparation of (1-x)$SrBi_2Ta_2O_9$-xBi_3TiTaO_9 thin films; strontium acetate, bismuth 2-ethylhexanoate, titanium isopropoxide and tantalum ethoxide were chosen as precursor, and acetic acid, 2-ethylhexanoic acid and 2-methoxyethanol were selected as solvents. Bismuth 2-ethylhexanoate and strontium acetate precursors were dissolved in 2-ethylhexanoic acid and acetic acid, respectively, under room temperature conditions. These solutions were then added to the solution of tantalum ethoxide in 2-methoxyethanol. Finally, titanium isopropoxide was added to prepare a stoichiometric (1-x)$SrBi_2Ta_2O_9$-xBi_3TiTaO_9

solution. The final solution was stirred for about 2 hr. before coating. The precursor solution was filtered through 0.2 μm syringe filters and then spin-deposited on to Pt-coated Si substrates at 6000 rpm for 1 min. After deposition, films were kept on a hot plate (at ~350 ^oC) in air for 10 min. to remove solvents and other organic and this step was repeated after each layer of coating to ensure complete removal of volatile matter. The post deposition annealing of the films was carried out in a furnace at different temperatures for one hour under oxygen environment. The thickness of the films was measured by variable angle spectroscopic ellipsometry. The (1-x)$SrBi_2Ta_2O_9$-xBi_3TiTaO_9 films of 0.25 μm thickness were used in this study. The structure of thin films was analyzed by x-ray diffraction (XRD). The diffraction patterns were recorded on a Scintag XDS 2000 diffractometer using CuK_α radiation (40 kV) at a scanning speed of 2° (2θ)/min. The surface morphology of the films was analyzed by Digital instrument's Dimension 3000 atomic force microscope (AFM) using tapping mode with amplitude modulation. The electrical measurements were conducted on films in metal-ferroelectric-metal (MFM) configuration using Pt as the top and bottom electrode. The Pt electrodes (area=3.1×10^{-4} cm^2) were deposited on the top surface of the films by sputtering through shadow mask. The films were annealed at 600 ^oC for 20 min. after top electrode deposition to ensure good electrical contact. Capacitance and tan δ values were measured with HP 4192A impedance analyzer at room temperature. Ferroelectric properties of the films were analyzed by RT66A ferroelectric test system. Leakage current vs. voltage characteristics were measured by means of a Keithley 617 electrometer/source.

3.4. RESULTS AND DISCUSSIONS

The properties of present solid solution thin films are discussed in three sections. First, the properties of (1-x)$SrBi_2Ta_2O_9$-xBi_3TiTaO_9 solid solution thin films are described in general. The effects of post-deposition annealing temperature and Bi_3TiTaO_9 content on the film properties have been analyzed. The properties of the optimum composition, established on the basis of structural, dielectric, and ferroelectric properties, are discussed in the second section. Finally, the feasibility of integration of present films directly on Si with PtRh/$PtRhO_x$ as electrode/barrier material has been demonstrated.

3.4.1. Properties of (1-x)$SrBi_2Ta_2O_9$-xBi_3TaTiO_9 solid solution thin films as a function of x

A. Structure and surface morphology

As pyrolyzed (1-x)$SrBi_2Ta_2O_9$-xBi_3TaTiO_9 thin films (at ~ 350 ^oC) were found to be amorphous in nature. The post-deposition annealing of the films was carried out in oxygen atmosphere to impart crystallinity. Figure 1 (a) shows the structure of (1-x)$SrBi_2Ta_2O_9$-xBi_3TaTiO_9 thin films as a function of Bi_3TaTiO_9 content x. The films were deposited on Pt-coated Si substrates and were of the same thickness. The films annealed at 750 ^oC exhibited a well crystallized phase with XRD patterns similar to that of $SrBi_2Ta_2O_9$ thin films [23]. There were no observable secondary phases present in the XRD patterns of films with up to 50% Bi_3TaTiO_9 content indicating the formation of complete solid solution. These results are consistent with those reported for bulk material [21]. The intensity and sharpness of (115) oriented peak was found to increase with increase in Bi_3TiTaO_9 content suggesting an increase in grain size for the solid solution compositions as compared to $SrBi_2Ta_2O_9$. The peaks in the XRD patterns were found to shift towards higher 2θ values with increasing Bi_3TiTaO_9 content. A similar trend was observed in bulk material which may possibly be due to substitutional replacement of Ti^{4+} for Ta^{5+} and Bi^{3+} for Sr^{2+} sites, respectively, causing a gradual change of unit cell dimensions [21]. Figure 1 (b) shows the typical effect of annealing temperature on the structure of 0.7$SrBi_2Ta_2O_9$-0.3Bi_3TaTiO_9 thin films. Similar XRD patterns were observed for films with up to 50% the Bi_3TaTiO_9 content. It was possible to obtain a pyrochlore free crystalline phase even at an annealing temperature of 600 ^oC. As the annealing temperature was increased, the peak intensity and sharpness was found to increase indicating an increase in crystallinity and grain size.

The surface morphology of the (1-x)$SrBi_2Ta_2O_9$-xBi_3TaTiO_9 thin films was analyzed by atomic force microscopy (AFM). Figure 2 shows the AFM micrographs of solid solution thin films as a function of x. The grain size was found to be significantly improved for the solid solution compositions as compared to $SrBi_2Ta_2O_9$ thin films [23]. These results are consistent with the XRD patterns where an increase in peak sharpness and intensity was observed with increasing Bi_3TaTiO_9 content. The surface morphology of solid solution thin films showed varying grain sizes as compared to $SrBi_2Ta_2O_9$ thin films exhibiting uniform grain distribution.

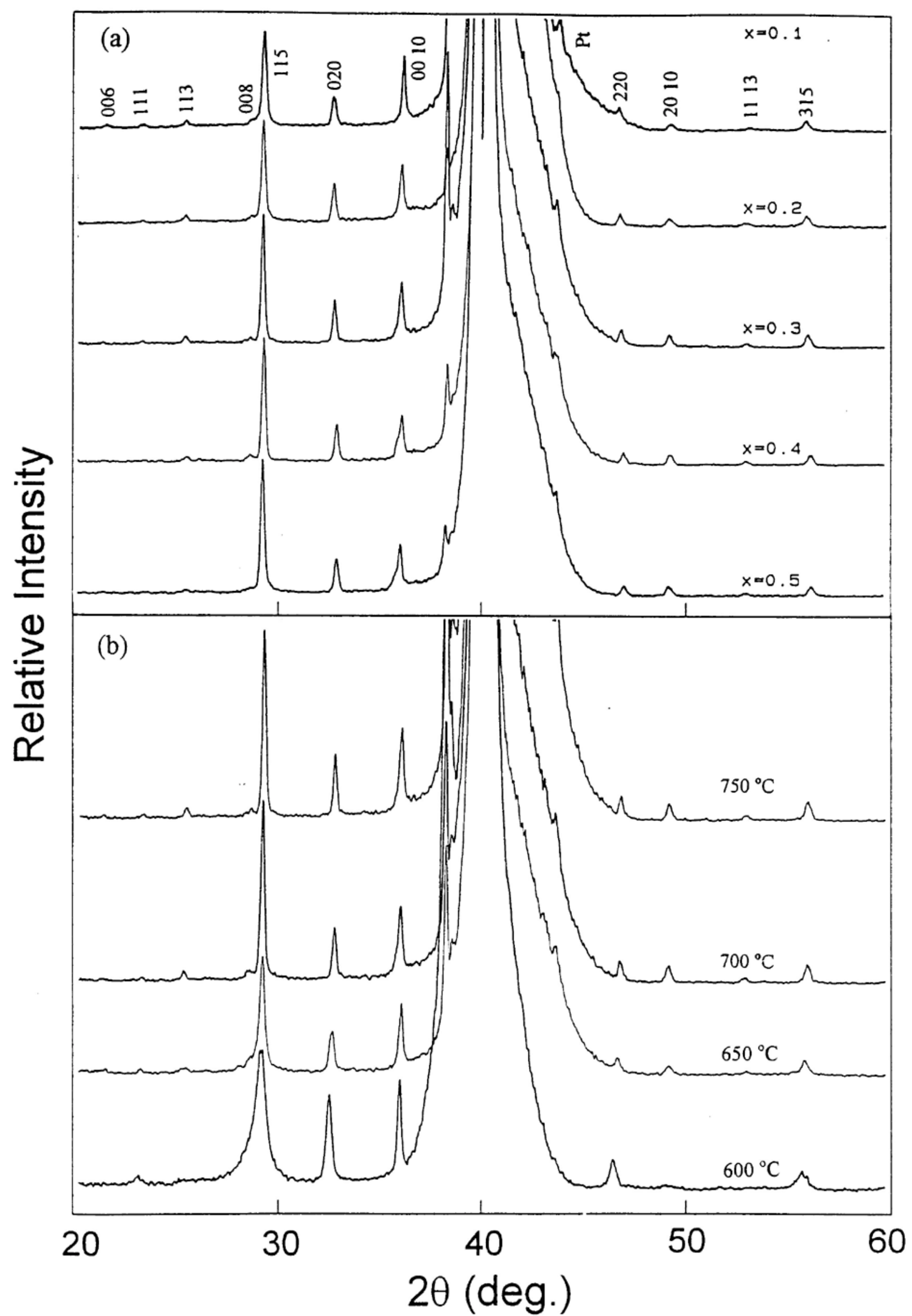

Figure. 3-1. X-ray diffraction patterns of (a) (1-x)$SrBi_2Ta_2O_9$-xBi_3TaTiO_9 thin films annealed at 750 °C for one hour as a function of x and (b) 0.7$SrBi_2Ta_2O_9$-0.3Bi_3TaTiO_9 thin films annealed at various temperatures for one hour.

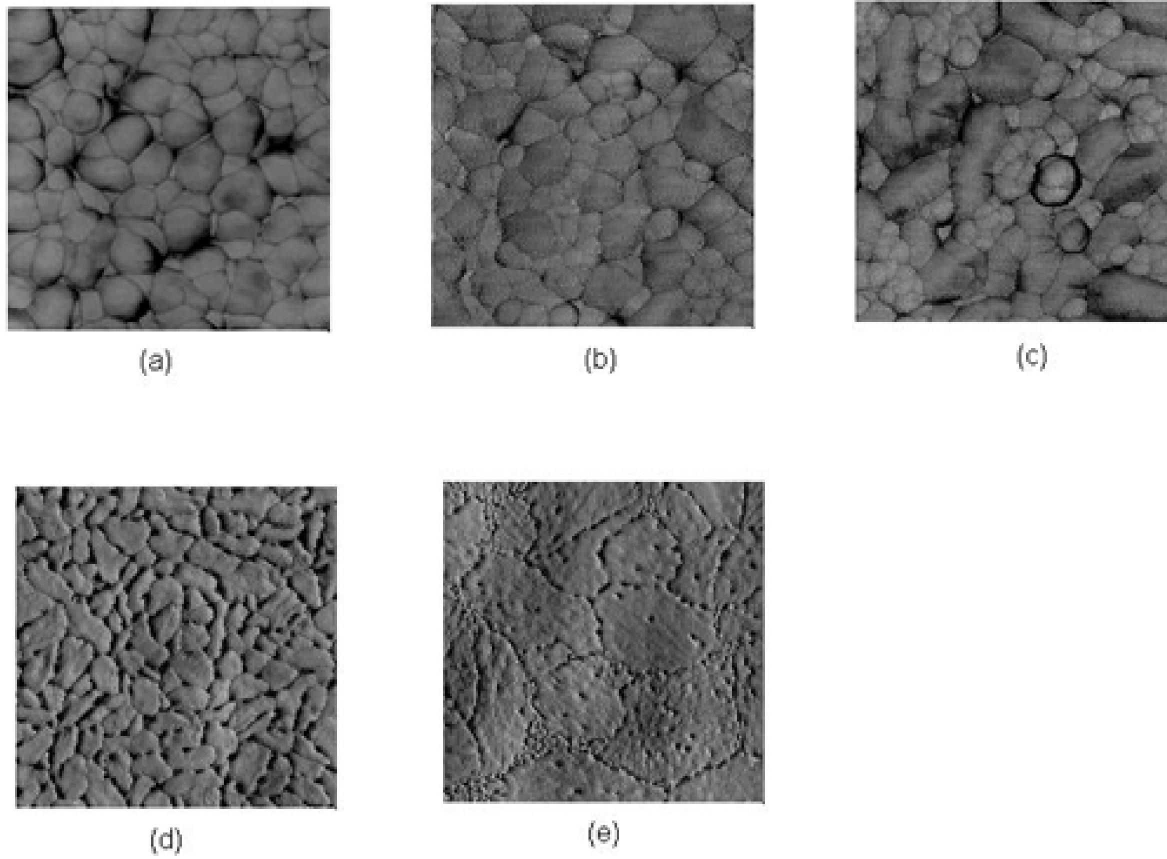

Figure. 3-2. AFM photographs of (1-x)$SrBi_2Ta_2O_9$-xBi_3TaTiO_9 thin films annealed at 750 °C for one hour. (a) x = 0.1, (b) x = 0.2, (c) x = 0.3, scanned in the area of 1 μm x 1μm, and (d) x = 0.4 (e) x = 0.5, in the area of 5 μm x 5 μm..

So, there may exist a second phase. The grain size variation was found to increase with increase in Bi_3TaTiO_9 content, however, the size and number of larger grains was found to increase. Figure 3 shows the typical effect of annealing temperature on the microstructure of $0.7SrBi_2Ta_2O_9$-$0.3Bi_3TaTiO_9$ thin films. The grain size was found to increase with increase in annealing temperature and showed significant enhancement, compared to $SrBi_2Ta_2O_9$, even at a low annealing temperature of 650 ^{o}C. The observed annealing temperature dependence is consistent with the XRD data showing sharper peaks at higher annealing temperatures. The enhanced grain growth for the solid solution compositions compared to $SrBi_2Ta_2O_9$ and its dependence on Bi_3TaTiO_9 content and annealing temperature show the possibility of obtaining good ferroelectric properties at lower annealing temperatures by optimizing the composition.

B. Dielectric properties

The dielectric properties of (1-x)$SrBi_2Ta_2O_9$-xBi_3TaTiO_9 thin films were analyzed in terms of dielectric constant ε_r and loss factor tan δ by applying a small ac signal of 10 mV amplitude. The amplitude of applied signal was kept low to minimize the domain wall contribution so that the dielectric constant obtained does not regard polarization state in the material. Figure 4 shows the dielectric response of Pt/(1-x)$SrBi_2Ta_2O_9$-xBi_3TaTiO_9/Pt capacitors as a function of x. The dielectric properties were measured at a frequency of 100 kHz. The dielectric constant was found to decrease with increase in Bi_3TaTiO_9 content and was in the range 180-225 for compositions with x =10-50%. The dielectric constant of solid solution thin films was found to be smaller than the value of 330 reported for $SrBi_2Ta_2O_9$ thin films [23]. The dielectric constant of bulk Bi_3TaTiO_9 material has been reported to be 100. So the solid solution of $SrBi_2Ta_2O_9$ and Bi_3TaTiO_9 material is expected to exhibit an intermediate dielectric constant value. The dissipation factor did not show any appreciable dependence on the Bi_3TaTiO_9 content and was lower than 3% for solid solution compositions at an applied frequency of 100 kHz.

C. Ferroelectric properties

Ferroelectric hysteresis measurements were conducted on (1-x)$SrBi_2Ta_2O_9$-xBi_3TaTiO_9 thin films in MFM configuration at room temperature using standardized RT66A ferroelectric test system. Figure 5 shows remanent polarization and coercive field of (1-x)$SrBi_2Ta_2O_9$-

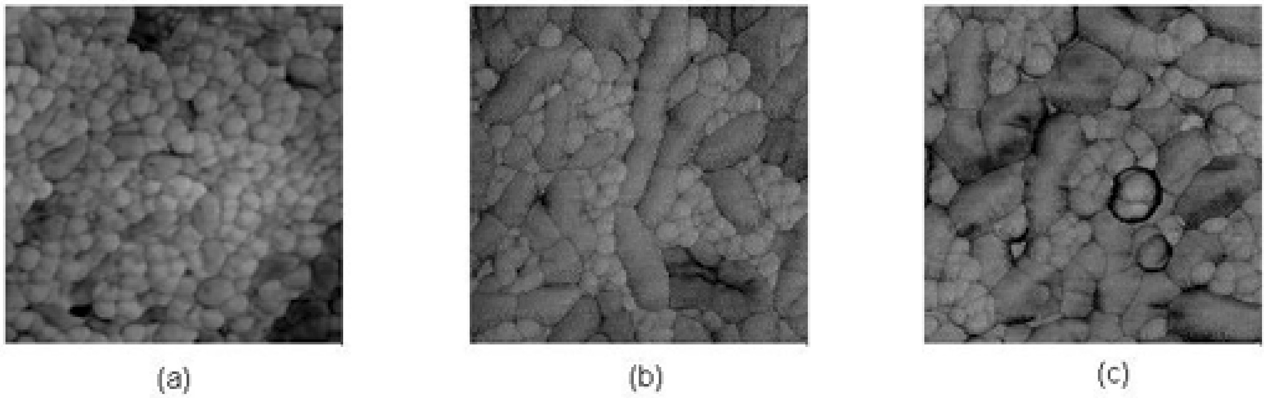

Figure. 3-3. AFM photographs of $0.7SrBi_2Ta_2O_9$-$0.3Bi_3TaTiO_9$ thin films annealed at (a) 650 ^oC, (b) 700 ^oC, and (c) 750 ^oC for one hour (scan area = 1 μm x 1 μm).

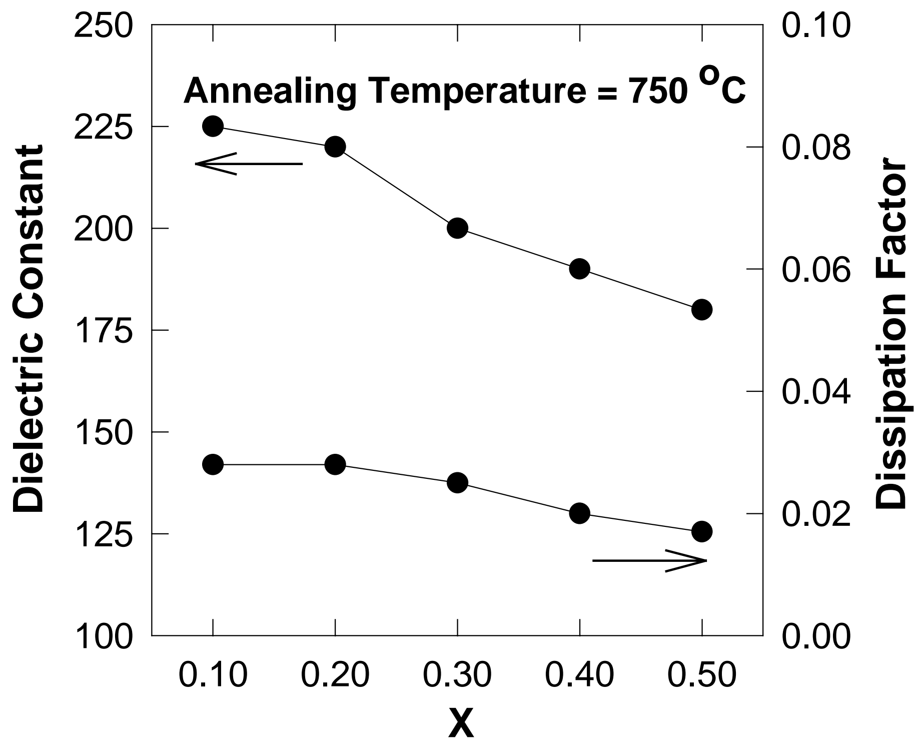

Figure. 3-4. Dielectric constant (ε_r) and Dissipation factor (tan δ) of (1-x)$SrBi_2Ta_2O_9$-xBi_3TaTiO_9 thin films annealed at 750 °C for one hour as a function of x.

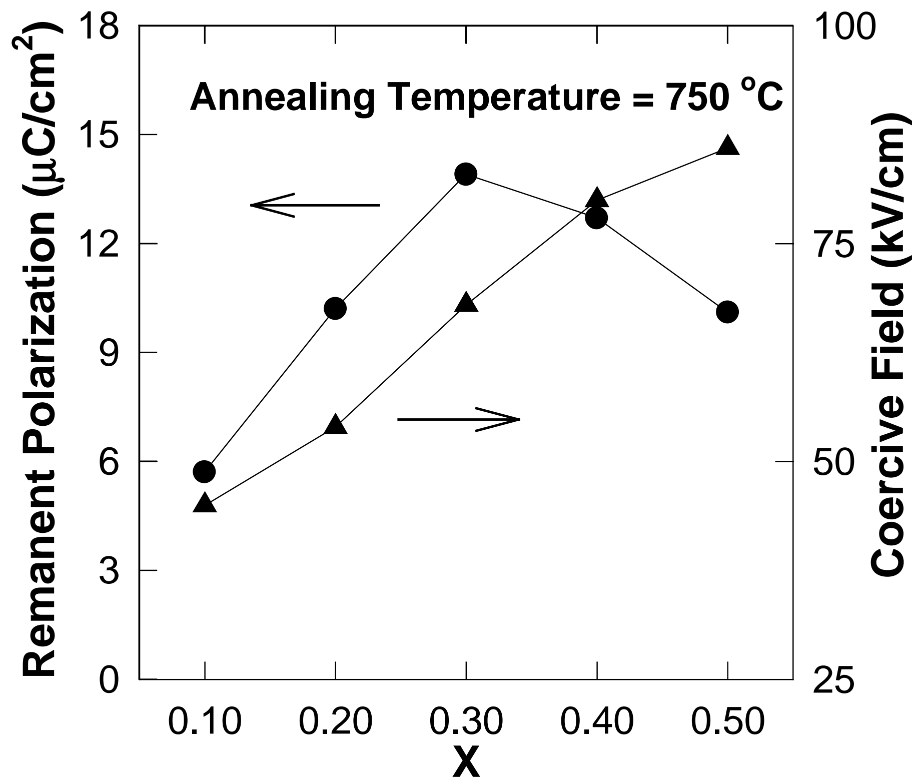

Figure. 3-5. Remanent polarization (P_r) and Coercive field (E_c) of (1-x)$SrBi_2Ta_2O_9$-xBi_3TaTiO_9 thin films annealed at 750 ^oC for one hour as a function of x.

xBi_3TaTiO_9 thin films, annealed at 750 °C, as a function of x. The P_r and E_c of solid solution thin films, measured at an applied electric field of 200 kV/cm, were in the range 5.7-13.9 μC/cm^2 and 45-86 kV/cm, respectively. The remanent polarization value showed a maximum for films with 30% Bi_3TaTiO_9 content while the coercive field was found to increase with increase in Bi_3TaTiO_9 content. The P_r value of solid solution thin films was found to be significantly improved compared to $SrBi_2Ta_2O_9$ thin films prepared under similar annealing temperature conditions [18,23]. The present results, higher P_r and larger grain size compared to $SrBi_2Ta_2O_9$, show the possibility of achieving good ferroelectric properties at lower annealing temperatures. The initial increase in remanent polarization, up to x=30%, was due to increase in grain size with increase in Bi_3TaTiO_9 content as was observed in AFM micrographs. However, the remanent polarization was found to decrease for samples with Bi_3TaTiO_9 contents larger than 30% even though the grain size was found to increase indicating that there may be other factors, apart from grain size, governing the ferroelectric properties of the (1-x)$SrBi_2Ta_2O_9$-xBi_3TaTiO_9 thin films. The observed decrease in P_r value may be due to increase in Curie temperature of solid solution compositions with increasing Bi_3TaTiO_9 content affecting the ferrolectric phase formation.

D. Fatigue and Retention characteristics

In general, bismuth layered-perovskite oxide materials, especially $SrBi_2Ta_2O_9$, show fatigue-free behavior under repeated switching which makes them attractive for memory devices. To investigate the fatigue properties of the system after incorporating Bi_3TaTiO_9, switching endurance of (1-x)$SrBi_2Ta_2O_9$-xBi_3TaTiO_9 thin film capacitor as a function of switching cycles was studied. The measurements were conducted at room temperature by applying 8.6-μs-wide bipolar pulses of 5 V amplitude. Figure 6 shows the degradation of the polarization state of the solid solution thin films as a function of x measured after 10^{10} polarization reversals. Up to 30 % Bi_3TaTiO_9 content, the switching degradation was less than 5% of its initial value. However, the films with 40-50% Bi_3TaTiO_9 content showed more than 10% decay in remanent polarization after 10^{10} switching cycles. The solid solution thin films showed a small decay in stored charge after 10^{10} switching cycles similar to $SrBi_2Ta_2O_9$ thin films [23]. Another parameter of importance for reliable long term operation of a memory device is the polarization charge retention. The retention measurements were also conducted using RT66A system. In the

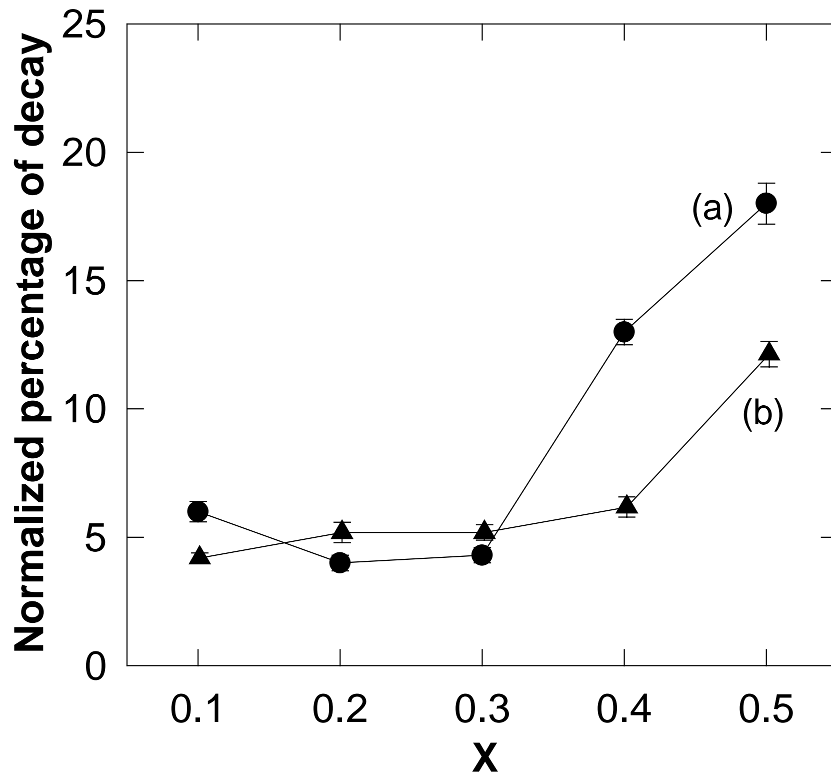

Figure. 3-6. Normalized percentage of decay in (a) remanent polarization after 10^{10} cycles of bipolar switching and (b) retained charge after 10^6 s. for (1-x)$SrBi_2Ta_2O_9$-xBi_3TaTiO_9 thin films annealed at 750 ^oC for one hour as a function of x.

measurement, the capacitor was initially poled with a negative voltage pulse, and the stored charge was read after a predetermined time interval by measuring the charge switched by a positive pulse. The measured retention behavior for solid solution thin films is shown in Fig 6. The decay in the retained charge was less than 5% of the initial value up to 10^6 seconds for films with up to 30% Bi_3TaTiO_9 content, which is a favorable behavior for memory applications. The small degradation of the retained charge and good polarization switching characteristics after 10^{10} cycles suggest the suitability of present (1-x)$SrBi_2Ta_2O_9$-xBi_3TaTiO_9 thin films for FRAM application.

E. Leakage current

The leakage current of ferroelectric oxide materials is a limiting factor for memory applications as the stored charge can leak through a capacitor due to excessive leakage current making the binary state unrecognizable. The leakage current behavior of (1-x)$SrBi_2Ta_2O_9$-xBi_3TaTiO_9 thin films was analyzed by applying dc voltages with a step of 0.5 V and a delay time of 60 seconds. The leakage current density of the films with up to 40% Bi_3TaTiO_9 addition, as shown in Fig. 7, was lower than 10^{-7} A/cm^2 up to an applied electric field of 200 kV/cm. However, the films with 50% Bi_3TaTiO_9 content showed significant increase in leakage current. The solid solution thin films with up to 40% Bi_3TaTiO_9 content showed leakage current density comparable to $SrBi_2Ta_2O_9$ thin films even though the grain size was significantly enhanced for the solid solution compositions. The observed increase in leakage current for films with 50% Bi_3TaTiO_9 content could be due to large amount of excess bismuth in the higher BTT mol%.

3.4.2. Properties of 0.7$SrBi_2Ta_2O_9$-0.3Bi_3TaTiO_9 thin films

The properties of solid solution thin films were found to be strongly dependent on the Bi_3TaTiO_9 content x. Based on structural, dielectric, ferrolectric, and leakage current studies on (1-x)$SrBi_2Ta_2O_9$-xBi_3TaTiO_9 thin films, 0.7$SrBi_2Ta_2O_9$-0.3Bi_3TaTiO_9 was identified as the optimum composition for FRAM applications. In this section, the properties of 0.7$SrBi_2Ta_2O_9$-0.3Bi_3TaTiO_9 thin films have been described in detail and a comparison has been made with

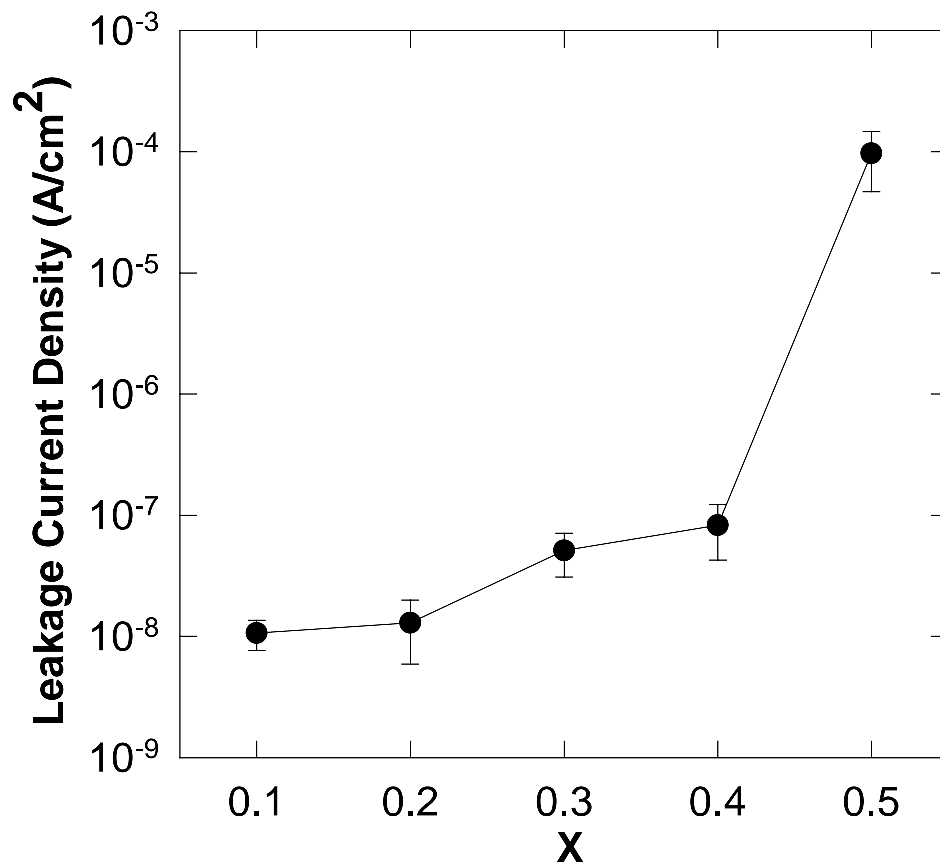

Figure. 3-7. Leakage current density of (1-x)$SrBi_2Ta_2O_9$-xBi_3TaTiO_9 thin films annealed at 750 ^oC for one hour as a function of x.

$SrBi_2Ta_2O_9$ thin film properties to establish their potential for memory devices. The structural, dielectric, and ferroelectric measurements were conducted on 0.25 μm thick films annealed in the temperature range 650-750 ^oC.

The dielectric response as a function of frequency provides important information about film/electrode interfacial characteristics. The dielectric measurements were conducted on MFM capacitors by applying a small ac signal of 10 mV amplitude to minimize domain contributions. Figure 8 shows the small signal dielectric constant and the dissipation factor, measured in the frequency range 1-1000 kHz, as a function of frequency for the $0.7SrBi_2Ta_2O_9$-$0.3Bi_3TaTiO_9$ thin films annealed at 750 ^oC for 1 hr. The measured dielectric constant and the dissipation factor at the frequency of 100 kHz were 200 and 0.025 respectively. The dielectric constant and dissipation factor did not show any appreciable dispersion up to 1 MHz, indicating good film/electrode interface characteristics and that the values were not coupled with any surface layer and/or electrode barrier effects in this frequency range. At frequencies higher than 1 MHz, the dielectric constant was found to decrease and loss factor was found to increase with frequency which was, possibly, due to L-C resonance effect at the terminals of the impedance analyzer as similar behavior was observed for thin films of other dielectric materials having similar order of capacitance [24]. The dielectric constant was found to increase with the increase in annealing temperature and was in the range 158-200 for films annealed in the temperature range 650-750 ^oC. The increase of dielectric constant with annealing temperature may be attributed to the improvement in crystallinity and grain size as was observed in XRD and AFM studies. The dissipation factor did not show any appreciable dependence on the annealing temperature.

As shown in Fig 9 (a), the $0.7SrBi_2Ta_2O_9$-$0.3Bi_3TaTiO_9$ thin films showed good ferroelectric P-E hysterisis loop even at an annealing temperature of 650 ^oC. The typical measured remanent polarization and coercive field values were 6.2 $\mu C/cm^2$ and 80 kV/cm, respectively, at an applied electric field of 200 kV/cm. The ferroelectric properties were significantly improved compared to $SrBi_2Ta_2O_9$ where no appreciable polarization charge is obtained at 650 ^oC. This is an encouraging result as processing temperatures lower than 700 ^oC are desirable for the selection of suitable electrode/barrier layers in between the ferroelectric film and silicon substrate. The remanent polarization value was found to increase with increase in annealing temperature and was in the range 6.2-13.9 $\mu C/cm^2$ for films annealed in the

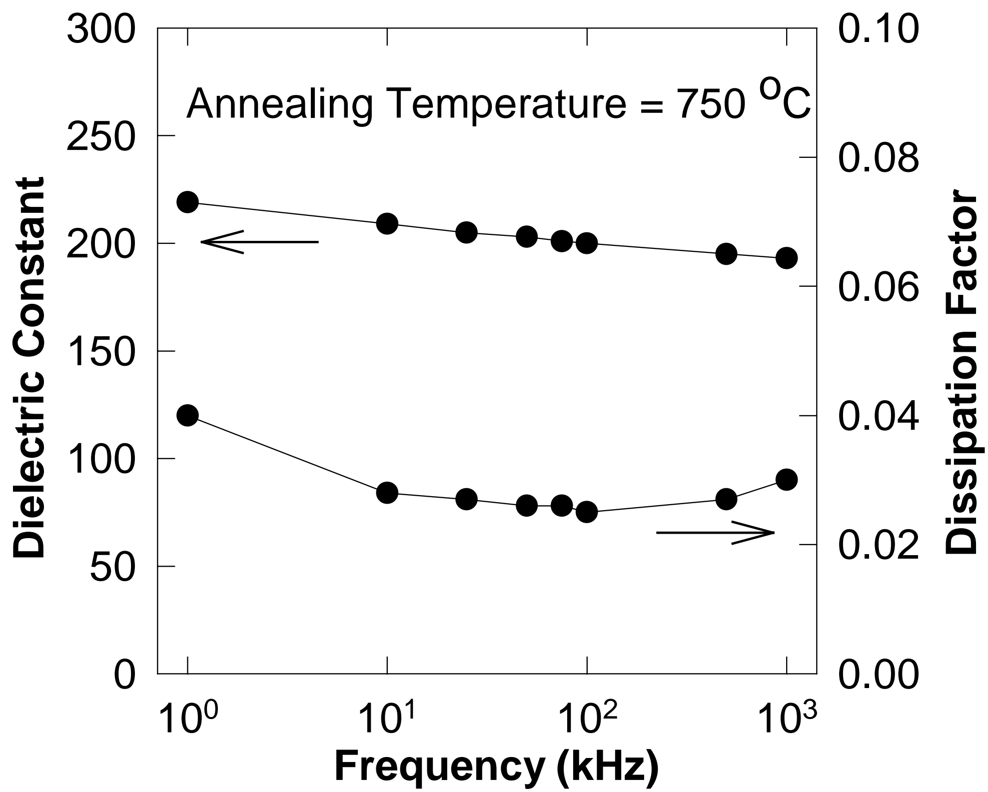

Figure. 3-8. Dielectric constant (ε_r) and Dissipation factor (tan δ) of $0.7SrBi_2Ta_2O_9$-$0.3Bi_3TaTiO_9$ thin films annealed at 750 ^oC for one hour as a function of frequency.

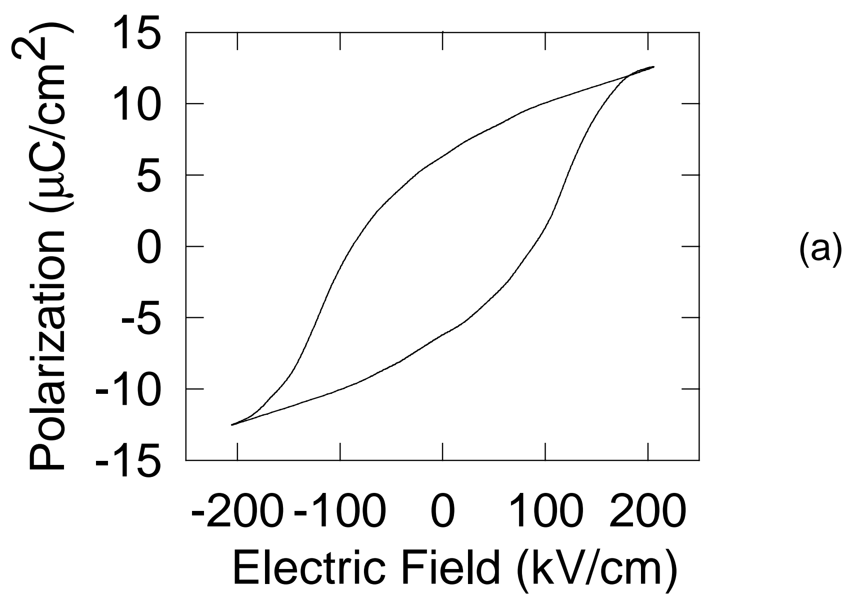

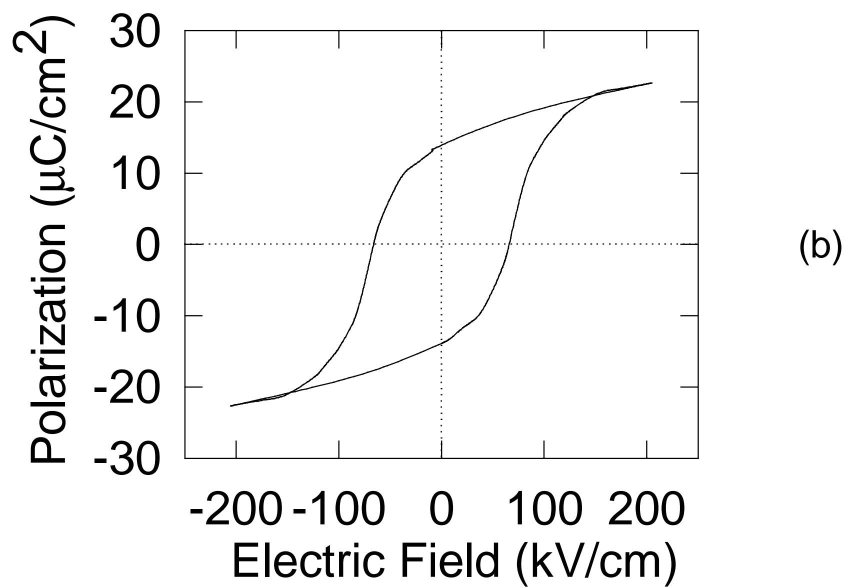

Figure. 3-9. Hysterisis loop of 0.25-μm-thick $0.7SrBi_2Ta_2O_9$-$0.3Bi_3TaTiO_9$ thin films annealed at (a) 650 ^oC and (b) 750 ^oC for one hour.

temperature range 650-750 ^{o}C. The solid solution thin film showed larger remanent polarization compared to $SrBi_2Ta_2O_9$ thin films which may be attributed to larger grain size of solid solution thin films. The significantly enhanced grain growth compared to $SrBi_2Ta_2O_9$ at an annealing temperature of 650 ^{o}C show the possibility of further reducing the processing temperature by optimizing the fabrication technique and processing conditions. The leakage current density of $0.7SrBi_2Ta_2O_9$-$0.3Bi_3TaTiO_9$ thin films, as shown in Fig. 10, was less than 10^{-7} A/cm^2 at the applied field of 200 kV/cm which is comparable to $SrBi_2Ta_2O_9$ thin films. The improved ferroelectric properties at lower annealing temperature and low leakage current density comparable to $SrBi_2Ta_2O_9$ thin films makes the present solid solution thin films attractive for high density integrated memory devices.

The reliability of $0.7SrBi_2Ta_2O_9$-$0.3Bi_3TaTiO_9$ thin films was analyzed in terms of fatigue and retention characteristics. Figure 11 shows the typical fatigue behavior for the $0.7SrBi_2Ta_2O_9$-$0.3Bi_3TaTiO_9$ thin films annealed at 750 ^{o}C. There was no decay in the polarization charge up to about 10^8 switching cycles which was then followed by a final decay period. Even after 10^{10} switching cycles, the decay in remanent polarization was observed to be less than 5% of initial value. Figure 12 shows the retention characteristics of $0.7SrBi_2Ta_2O_9$-$0.3Bi_3TaTiO_9$ thin films annealed at 750 ^{o}C for 1 hr. The decay in the retained charge was less than 5% even after a retained time of 10^6 seconds. The good fatigue and retention properties of the $0.7SrBi_2Ta_2O_9$-$0.3Bi_3TaTiO_9$ thin films, comparable to $SrBi_2Ta_2O_9$ thin films, establish their reliability for FRAM applications.

3.4.3. Integration of $0.7SrBi_2Ta_2O_9$-$0.3Bi_3TaTiO_9$ thin films on metal-oxide electrodes

For high density FRAM applications, the ferroelectric thin film needs to be deposited on poly-Si plug. The integration on poly-Si plug requires a suitable electrode/barrier layer stable up to the processing temperature of the ferroelectric film. Annealing at temperatures lower than 700 ^{o}C is desirable for the selection of a stable electrode/barrier material. Recently, Pt-RhO_x has been proposed as a suitable electrode/barrier material for the integration of PZT films on silicon substrate. In the present work we have made an attempt to deposit $0.7SrBi_2Ta_2O_9$-$0.3Bi_3TaTiO_9$ thin films on Si with Pt-RhOx as electrode/barrier layer. The 0.1-µm-thick films were deposited on Pt-10%Rh/Pt-RhO_x/n^+-poly Si substrates. The films were annealed in an oxygen environment at 650 ^{o}C for 1hr. The hysterisis loop measurements were conducted using Pt-10%Rh as top

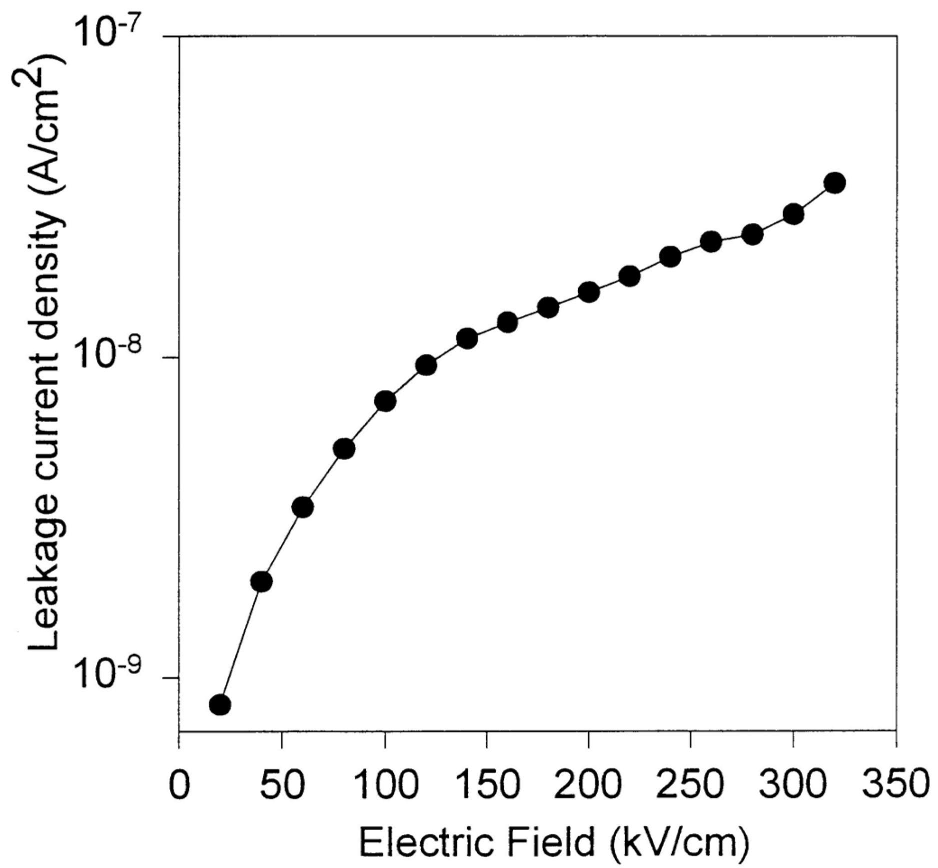

Figure. 3-10. Leakage current density vs. electric field characteristic of $0.7SrBi_2Ta_2O_9$-$0.3Bi_3TaTiO_9$ thin films annealed at 750 °C for one hour.

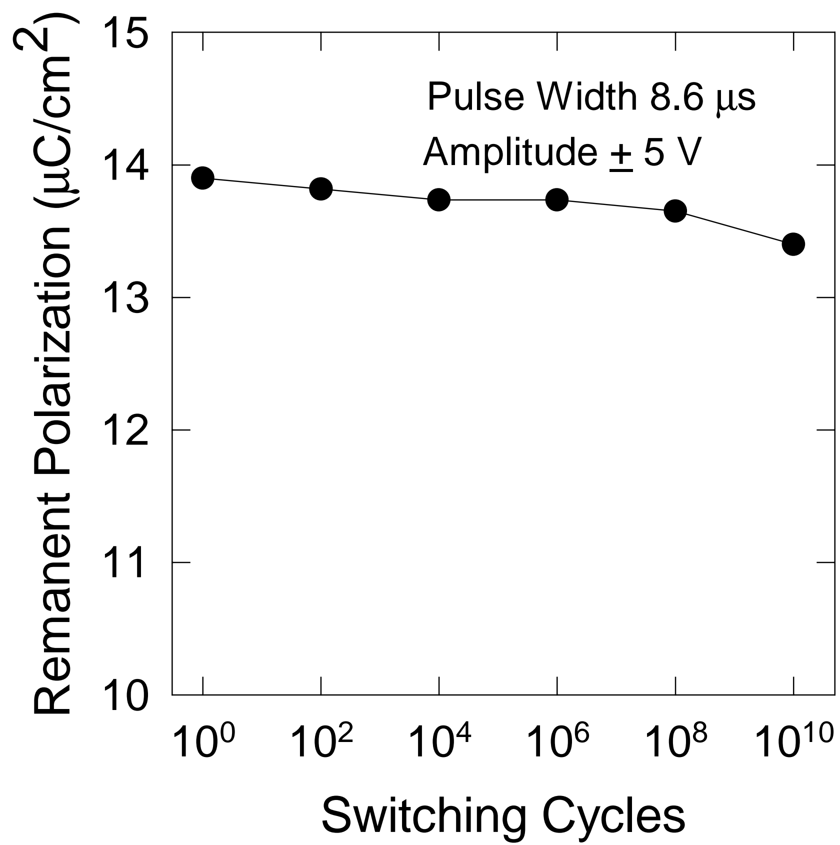

Fig. 3-11. Fatigue characteristics of $0.7SrBi_2Ta_2O_9$-$0.3Bi_3TaTiO_9$ thin films annealed at 750 ^oC for one hour.

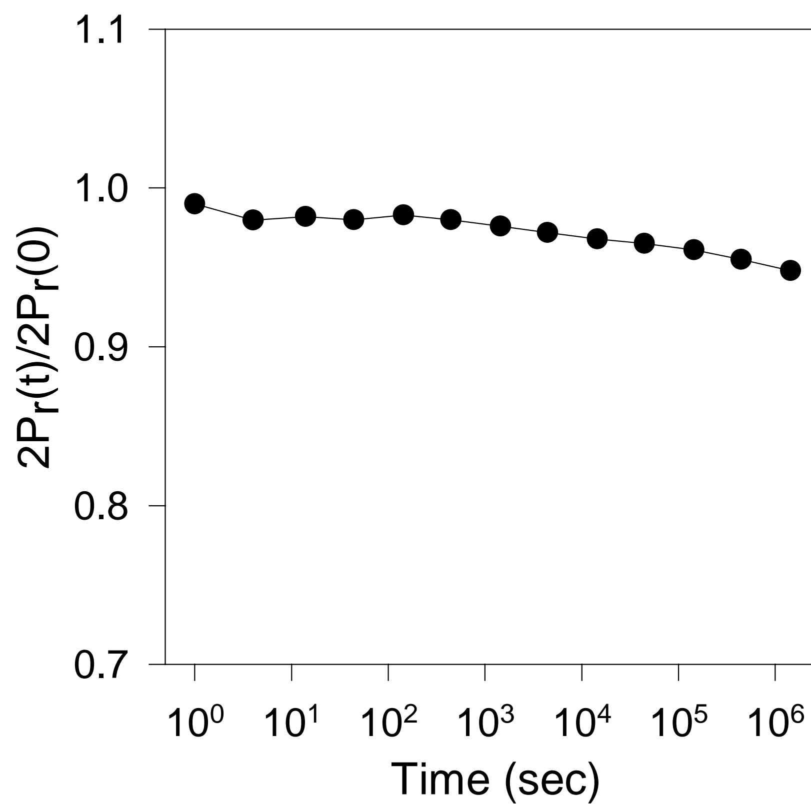

Fig. 3-12. Normalized retention characteristics of $0.7SrBi_2Ta_2O_9$-$0.3Bi_3TaTiO_9$ thin films annealed at 750 ^oC for one hour.

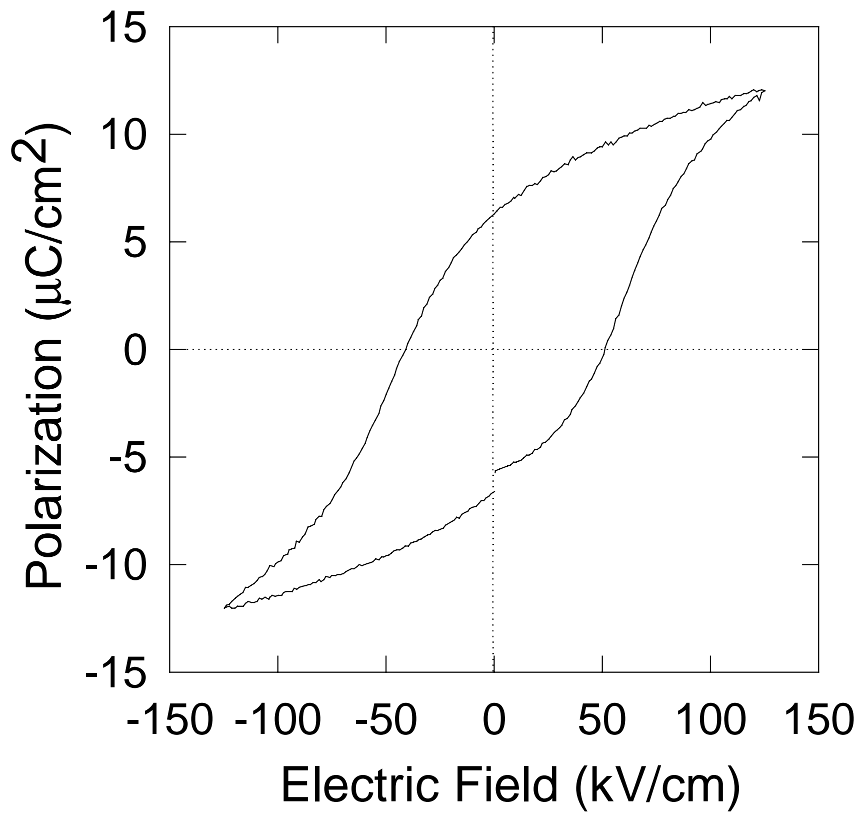

Fig. 3-13. Hysterisis loop of 0.1-μm-thick $0.7SrBi_2Ta_2O_9$-$0.3Bi_3TaTiO_9$ thin films annealed at 650 °C for one hour on Pt-10%Rh/$PtRhO_x$/n^+-poly Si substrate.

electrode. Figure 13 shows the typical P-E hysteresis loop of $0.7SrBi_2Ta_2O_9$-$0.3Bi_3TaTiO_9$ thin film measured by applying 3V between top electrode and n^+-poly Si. The typical measured remanent polarization and coercive field, as shown in Fig. 13, were 5.6 $\mu C/cm^2$ and 50 kV/cm, respectively. The $0.7SrBi_2Ta_2O_9$-$0.3Bi_3TaTiO_9$ solid solution thin films successfully deposited on Pt-RhOx electrode/barrier material with good ferroelectric hysteresis properties at a low annealing temperature of 650 ^oC promise to solve major process compatibility problems with $SrBi_2Ta_2O_9$ for the realization of commercially viable nonvolatile FRAM devices.

3.5. CONCLUSIONS

(1-x)$SrBi_2Ta_2O_9$-xBi_3TaTiO_9 solid solution thin films were successfully deposited on platinum coated silicon substrates by MOSD technique using alkoxide-salt precursors. The solid solution thin films exhibited superior ferroelectric properties compared to $SrBi_2Ta_2O_9$ thin films. The microstructure and electrical properties of the films were found to be strongly dependent on the Bi_3TaTiO_9 content. The grain size was found to be significantly enhanced for the solid solution compositions even at a low annealing temperature of 650 ^oC. Based on the structural, dielectric, and ferroelectric properties, $0.7SrBi_2Ta_2O_9$-$0.3Bi_3TaTiO_9$ was identified as the optimum composition for FRAM applications. A high remanent polarization of 13.9 $\mu C/cm^2$ was obtained for the optimum composition at an annealing temperature of 750 ^oC. It was possible to obtain good ferroelectric properties even at a low annealing temperature of 650 ^oC due to enhanced grain growth as compared to $SrBi_2Ta_2O_9$. The typical measured P_r for $0.7SrBi_2Ta_2O_9$-$0.3Bi_3TaTiO_9$ thin films annealed at 650 ^oC was 6.2 $\mu C/cm^2$. The observed dielectric constant and loss factor for $0.7SrBi_2Ta_2O_9$-$0.3Bi_3TaTiO_9$ thin film annealed at 750 ^oC were 200 and 0.025, respectively. The films showed good fatigue characteristics under bipolar stressing up to 10^{10} switching cycles. The loss in retained charge was only 10% range of its initial value and leakage current density was lower than 10^{-7} A/cm^2 up to an applied electric field of 200 kV/cm suggesting the suitability of $0.7SrBi_2Ta_2O_9$-$0.3Bi_3TaTiO_9$ thin films for FRAM applications. It was possible to obtain good ferroelectric properties on 0.1 μm-thick $0.7SrBi_2Ta_2O_9$-$0.3Bi_3TaTiO_9$ thin films deposited on Pt-RhO_x/Si substrates. A remanent polarization of 5.6 $\mu C/cm^2$ and coercive field of 50 kV/cm were obtained at an annealing temperature of 650 ^oC which makes the solid solution thin films attractive for high density

memory applications. The microstructural and ferroelectric studies suggest that (1-x)$SrBi_2Ta_2O_9$-xBi_3TaTiO_9 thin films have great potential to overcome the obstacles which $SrBi_2Ta_2O_9$ thin films, especially, for the realization of a practical memory device.

3.6 REFERENCES

[1] J.F. Scott, C.A. Araujo, Science 246 (1989) 1400.

[2] S. Dey, R. Zuleeg, Ferroelectrics 108 (1990) 37.

[3] R. Moazami, C. Hu, W.H. Shepherd, IEEE Trans. Electronic Devices 39 (1992) 2044.

[4] J.F. Scott, C.A. Araujo, H.B. Meadows, L.D. McMillan, A. Shawabkeh, J. Appl. Phys. 66 (1989) 1444.

[5] S. Sinharoy, H. Buhay, D.R. Lampe, M.H. Francombe, J. Vac. Sci. Technol. A10 (1992) 1554.

[6] V.S. Postnikov, V.S. Pavlov, S.A. Gridnev, S.K. Turkov, Soc. Phys. Solid St. 10 (1968) 1267.

[7] H.N. Al-shareef, A.I. Kingon, X. Chen, K.P. Bellur, O. Auciello, J. Mater. Res. 9 (1994) 2968.

[8] I.K. Yoo, S.B. Desu, J. Xing, Mater. Res. Soc. Symp. Proc. 310 (1993) 165.

[9] R. Ramesh, W.K. Chan, B. Wilkens, H. Gilchrist, T. Sands, J.M. Tarascon, V.G. Keramidas, D.K. Fork, J. Lee, A. Safari, Appl. Phys. Lett. 61 (1992) 1537.

[10] H.N. Al-shareef, O. Auciello, A.I. Kingon, J. Appl. Phys., 77 (1995) 2146.

[11] C.A. Araujo, J.D. Cuchlaro, L.D. McMillan, M.C. Scott, J.F. Scott, Nature 374 (1995) 627.

[12] K. Amanuma, T. Hase, Y. Miyasaki, Appl. Phys. Lett. 66 (1995) 221.

[13] S.B. Desu, D.P.Vijay, Mater. Sci. Eng. B32 (1995) 75.

[14] K. Amanuma, T. Hase, Y. Miyasaka, Mater. Res. Soc. Symp. Proc. Ferroelectric Thin Films IV (Materials Research Symposium, Pittsburgh) 1995, 21.

[15] S. Ohnishi, K. Ishihara, Y. Ito, S. Yokoyama, J. Kudo, K. Sakiyama, IEDM Tech. Digest 94 (1994) 843.

[16] G. Arlt, D. Hennings, G. Dewith, J. Appl. Phys. 58 (1985) 1619.

[17] S.B. Desu, C.H. Peng, L. Lammerdiner, P.J. Schuele, Mater. Res. Soc. Symp. Proc. 200

(1990) 319.

[18] T. Noguchi, T. Hase, Y. Miyasaka, Jpn. J. Appl. Phys. 35 (1996) 4900.

[19] Y. Ito, M. Ushikubo, S. Yokoyama, H. Matsunaga, T. Atsuki, T. Yonezawa, K. Ogi, Jpn. J. Appl. Phys. 35 (1996) 4925.

[20] E.C. Subbarao, J. Chem. Phys. 34 (1961) 695.

[21] X. Zhang, P. Gu, S.B. Desu, Phys. Stat. Sol. (a)160 (1997) 35.

[22] K. Singh, D.K. Bopardikar, D.V. Atkare, Ferroelectrics 82 (1988) 55.

[23] P.C. Joshi, S.O. Ryu, X. Zhang, S.B. Desu, Appl. Phys. Lett. 70 (1997) 1080.

[24] P. C. Joshi, S. B. Desu, J. Appl. Phys. 80 (1996) 2349.